Journal of Radiation Research and Applied Sciences 17 (2024) 101175

Contents lists available at ScienceDirect

Journal of Radiation Research and Applied Sciences

journal homepage: www.journals.elsevier.com/journal-of-radiation-research-and-applied-sciences

Mechanical properties and radiological implications of replacing sand with waste ceramic aggregate in ordinary concrete

I.O. Olarinoye [a,*], M.T. Kolo [a], D.B. Amuda [b], C.O. Oche [a], B. Mohammed [a], Jamila S. Alzahrani [c], M.S. Al-Buriahi [d,**]

[a] Department of Physics, Federal University of Technology, Minna, Nigeria
[b] Department of Pure and Applied Physics, Ladoke Akintola University of Technology, Ogbomoso, Oyo State, Nigeria
[c] Department of Physics, College of science, Princess Nourah bint Abdulrahman University, P.O. Box 84428, Riyadh 11671, Saudi Arabia
[d] Department of Physics, Sakarya University, Sakarya, Turkey

ARTICLE INFO

Keywords:
Aggregates
Compressive strength
Concrete
Natural radionuclides
Waste ceramic tiles

ABSTRACT

The mining of aggregates for the production of concrete creates ecological problems. In this study, the effect of partially replacing sand as fine aggregate (FA) with waste ceramic tiles (WCT) on the density, compressive strength (CS), specific radioactivity of naturally occurring radioactive materials (^{238}U, ^{232}Th, and ^{40}K), and the radiation shielding competence of concrete was investigated. Ordinary concrete samples consisting of cement, fine aggregate (river sand), coarse aggregate (granite), and water were prepared in 50 mm × 50 mm x 50 mm cubical steel moulds. The samples were coded as C-WCT0, C-WCT5, C-WCT10, C-WCT15, C-WCT20, and C-WCT25, representing concrete samples in which the FA component was replaced by 0, 5, 10, 15, 20, and 25% pulverized WCT, respectively. The CS and density of the samples were determined after 7-, 14-, and 28-day curing periods. The gamma spectrometric method was used to determine the specific activity of ^{238}U, ^{232}Th, and ^{40}K using a hyper pure germanium detector. The photon and neutron shielding parameters of the concrete blocks were calculated with the aid of the EPICS2017 cross-section library and relevant standard formulae. The mean CS for each concrete category increase with curing age. The density of the concrete varied from 2213 kg/m^3 to 2488 kg/m^3 as the FA replacement level rose to 15%. Using WCT as a partial replacement for FA altered the chemical composition and decreased the specific activities of ^{238}U, ^{232}Th, and ^{40}K, in the concrete samples. C-WCT15 had the best gamma photon and fast neutron absorption features among the concrete samples. The use of WCT as aggregate in concrete production is a sustainable and environmental-friendly way of producing concrete for general civil engineering and shielding applications in medical and other radiation facilities. This study also affirms that using alternative materials with lower specific activity to replace sand is radiologically desirable in reducing the indoor radiation dose of occupants of concrete-based structures. The replacement of 15% sand by WCT produced stronger, radiologically safer, and more effective radiation absorbing concrete.

1. Introduction

The characterisation of concrete is crucial in structural engineering and radiological applications. Concrete is a common and versatile building material whose applications cut across ages, economic strata, and countries. The need to provide homes, offices, roads, and other civil engineering structures for the growing global population has made the demand for concrete increase over the years. However, the production of concrete comes at a huge environmental cost. Traditionally, concrete is a composite material that is made from a mixture of cement, aggregates, and water. These raw materials are derived from geological formations; therefore, harvesting them for the purpose of concrete production creates environmental-related problems. For example, the production of cement has been reported to contribute significantly to the emission of CO_2, a greenhouse gas, and thus to global warming (Kanthe, 2021; Singh et al., 2020). Aside from CO_2, the production of cement is also associated with the release of dust and poisonous gases that pollute the ambient air (Mansour et al., 2023). Aggregates, on the hand,

* Corresponding author.
** Corresponding author.
E-mail addresses: leke.olarinoye@futminna.edu.ng (I.O. Olarinoye), alburiahi@sakarya.edu.tr (M.S. Al-Buriahi).

https://doi.org/10.1016/j.jrras.2024.101175
Received 21 September 2024; Received in revised form 25 October 2024; Accepted 4 November 2024
Available online 8 November 2024
1687-8507/© 2024 The Authors. Published by Elsevier B.V. on behalf of The Egyptian Society of Radiation Sciences and Applications. This is an open access article under the CC BY-NC-ND license (http://creativecommons.org/licenses/by-nc-nd/4.0/).

constitute at least 70% by volume in a typical concrete sample. A simple construction could consume about 200 tons of sand, while a 10-km road requires about 30 kilotons of sand (Rentier & Cammeraat, 2022). As long as there are needs for concrete-based houses and other civil engineering structures, the demand for aggregates will continue to rise worldwide. Within the last century, it was reported that the global demand for sand rose more than 20 times and was projected to exceed 80 billion tons by 2060 (Fritts, 2019; Rentier & Cammeraat, 2022; Torres et al., 2017). Consequently, the problems associated with the sourcing of sand are expected to be on the rise as well. Due to water being an agent of transportation for sediments, sand is often mined from waterbodies such as rivers and coasts. This causes riverbed degradation due to changes in the shape and formation of riverbeds. These indirectly cause a host of environmental hazards that threaten lives and biodiversity. In addition, the direct mining of sand from the earth's surface has immensely contributed to environmental challenges such as erosion, flooding, and associated problems that pose a threat to lives, property, and the ecosystem (Zhang, Sun, et al., 2023). It is therefore important from an environmental sustainability perspective that alternative and eco-friendly materials be used for concrete making. This will reduce the impact of sand mining and sourcing for other raw materials required for concrete making on the environment.

As part of efforts aimed at reducing the economic cost and environmental impacts of sourcing sand for concrete making, many materials such as furnace slag, waste plastics, recycled concrete, waste ceramics tyles etc. have been suggested for partial sand replacement in concrete making. In addition, the effects of replacing sand (fine aggregate (FA)) with more environmentally friendly alternative materials on the quality of concrete has been extensively investigated (Al- et al., 1997; Awoyera et al., 2018; Bhardwaj et al., 2023a; Ismail & Al-Hashmi, 2008; Lopez et al., 2007; Saikia & De Brito, 2014; Thorneycroft et al., 2018; Zhang, Shen, et al., 2023). For instance, recycled waste plastic, which is non-biodegradable and an environmental nuisance, was investigated as a partial replacement for sand in many previous studies (Al- et al., 1997; Ismail & Al-Hashmi, 2008; Khaleel et al., 2024; Saikia & De Brito, 2014; Thorneycroft et al., 2018) with promising outcomes. According to Manaseer and Dalal (Al- et al., 1997), using waste plastics as a partial replacement for sand reduced the compressive strength (CS) of concrete. This was attributed to the low bonding interaction between the plastic and cement mortar. In addition to the reduction in CS, the concrete density was also found to reduce in other studies (Ismail & Al-Hashmi, 2008; Saikia & De Brito, 2014). Thorneycroft et al. (Saikia & De Brito, 2014) also opined that a sand replacement level of 10% by volume of recycled plastic waste with a comparable particle size as sand, a rough surface, and an irregular shape is potentially promising for the production of viable and cost-effective concrete that could save about 800 million tons of sand globally. Recently, Bhardwaj et al. (Bhardwaj et al., 2023a) presented a comprehensive review on the effects of using waste furnace slag as a partial replacement for sand as fine aggregate on the different properties of concrete, such as workability, water requirement during mixing, etc. They found that, increasing the replacement level to 30% caused a reduction in workability and water content. In addition, the influence of the furnace slag on concrete strength depends on its proportion in the concrete. For instance, for replacement levels between 30 and 50%, the CS increased. On the other hand, the CS decreased for replacement levels outside this range. Ali et al. (Ali et al., 2022) Consider the use of recycled aggregate as a replacement for natural and fresh aggregate, as a way of mitigating the influence of extracting natural aggregate for concrete production on the environment. Unfortunately, the recycled aggregate produced concrete with inferior properties compared to those produced from fresh aggregate. Other studies have also shown that recycled aggregate may not significantly change the structural properties of concrete at low doses, but a high dose of more than 50% replacement level could negatively influence the strength and durability of concrete (Ahmadi et al., 2017; Kaplan et al., 2021; Kurda et al., 2018). The properties of concrete made from recycled aggregates have also been analysed and predicted based on different machine learning algorithms by (Ibrahim et al., 2023; Omer et al., 2024). In another investigation, Mishra et al. (Mishra et al., 2016) showed that partially replacing FA with granulated furnace slag produced durable concrete with low early-age shrinkage. The results from these aforementioned studies indicated that the nature and proportion of the replacement material is a strong factor that determines the properties of concrete. Ceramic aggregate is a light-weight, poor heat and electricity conductor, low-cost, and can act as another green replacement for sand in concrete. In 2016, Awoyera et al. (Awoyera et al., 2018) showed that the use of ceramic aggregate improved the different strength parameters of concrete. In a related study, Zhang et al. (Zhang, Shen, et al., 2023) showed that replacing sand between 20 and 100% with ceramic waste tile aggregate had profound effects on the properties of concrete. The research showed that a replacement level of 100% produced concrete with enhanced CS and flexural strength after 28 days of curing. However, the sustainability of such concrete could not be guaranteed due to the higher ratio of concrete demand to waste ceramic tiles generation. Earlier, Lopez et al. (Lopez et al., 2007) had shown that there was no considerable alteration in the mechanical properties of concrete when 10–50% of river sand is replaced with white ceramic powder.

Ceramic waste is generated as a result of destruction of ceramic product, renovation of buildings, as well as in the production process. The use of waste material in concrete production serves at least three purposes. First, it provides a safe way of disposing of waste materials and thus makes the environment cleaner and safer. Second, it reduces the volume of pristine materials required for concrete production, thus conserving natural resources and protecting the environment. Finally, using waste materials is more economical and eco-friendlier. These benefits could be consolidated if the produced concrete met the demands of civil engineering quality. Moreso, the applications of such concrete could be extended to nuclear radiation shielding purposes if their shielding competence increases as a result of the material replacement. However, many of the previous studies have concentrated on the influence of the replacement of aggregates with other materials on the physical and mechanical properties of concrete. Studies on the radiological impacts of such replacements are scarce. Cements, aggregates, and water are geological materials; they thus contain naturally occurring radionuclide materials (NORMs) in varying degrees. The extent of the NORMs (^{238}U, ^{232}Th, and ^{40}K) in a concrete sample thus depends on the radionuclide content of the composition (aggregates and cement) of the concrete (Olarinoye et al., 2023). Consequently, as a conventional radiation shielding material (RSM) (used in radiation facilities found in hospitals, research facilities, and nuclear power plants, among others), a high NORM concentration is undesirable as the concrete shield itself becomes a source of radiation. As a building material, high NORM content poses a health risk to inhabitants, as walls and other parts of the building made from concrete constitute major sources of indoor radiation. Consequently, concrete designed for buildings should not only be tested based on mechanical strength and other civil engineering qualities but should also be examined for natural radioisotope content and, their radiation shielding competences. High-radiation-absorbing concrete could be deployed for home construction in high-radiation areas and for providing shelters in nuclear accident scenarios. They could also serve as RSMs in facilities where ionizing radiation are employed.

In this study, the influence of substituting sand with waste ceramic on the CS, NORM concentrations, and shielding efficacy of concrete is investigated. This research evaluates the mechanical as well as the radiological consequences of replacing sand with waste ceramics with the objective of ascertaining the usefulness of the concrete as a civil engineering material as well as in radiation environments. The objective of this study is to examine the structural and radiological fitness of concrete produced using recycled ceramic tiles as fine aggregate. This research thus attempts to provides empirical evidence on the use of

waste ceramic tiles as alternative, green, and sustainable partial substitute for natural aggregates in concrete making. Although many synthetic materials including glasses (Al- et al., 2021; Al- et al., 2022; Alalawi et al., 2020; Alzahrani et al., 2022; Olarinoye et al., 2020) have been recommended for shielding applications, the produced concrete samples in this study are useful for general engineering applications and as biological shielding materials.

2. Materials and method

2.1. Concrete preparation

Ordinary concrete samples consisting of Ordinary Portland Cement (OPC), fine aggregate (FA) (river sand), coarse aggregate (CA) (granite), and water were prepared in conformity with the ASTM standards (Olarinoye et al., 2021; Qaidi et al., 2022; Tayeh et al., 2022). River sand and granite chips were obtained locally around the Minna area of Nigeria, while the cement (OPC) used was obtained from the open market in the same area. Sand of minimum grain size of 600 μm was used in preparing the concrete. Waste wall ceramic tiles (WCT) were collected, pulverized to pass through 600 μm mesh size, was used as a partial replacement for sand in the preparation of the concrete samples. Fine (sand/pulverized WCT) and coarse aggregates were blended without water for about 5 min, after which an appropriate amount of cement was added and further mixed for another 10 min to obtain a homogenous mix. Tap water was then introduced into the mix, which was further mixed for another 2 min. A consistent water/cement ratio of about 0.5 by weight was used for the concrete samples. Also, a ratio of 1:2:2 for cement: fine aggregate: coarse aggregate was adopted for the concrete samples. A summary of the concrete mixture is presented in Table 1. For all the concrete samples, a polycarboxylate-based superplasticizer was added to the mixture at an average of 1 wt% of the cement dosage. Six concrete samples coded as C-WCT0, C-WCT5, C-WCT10, C-WCT15, C-WCT20, and C-WCT25, representing concrete samples in which the sand component was replaced by 0, 5, 10, 15, 20, and 25%, respectively, were prepared. The freshly prepared samples were poured into 50 mm × 50 mm x 50 mm cubical steel moulds. The moulds were placed on a concrete vibrator for 10 min to allow compactness, reduce voids or air bubbles, and give shape. The cubes were de-moulded after 24 h and cured in a tank filled with water at 25 °C before further tests. The summary of the concrete preparation and further test and analysis is given in Fig. 1.

2.2. Compressive strength test and density

A compressive strength test was carried out on the concrete cubes in triplicate after a 7-, 14-, and 28-day curing period following the ASTM C109 standard procedure (ASTM C 109/C 109M and – 08, 2008). In addition, the density of each concrete sample was measured after 7, 14, and 28 days of curing. Fig. 2 shows the compressive test process, internal structure of the concrete and mass measuring routine.

Table 1
Concrete mixture proportion.

Concrete sample	Concrete composition (kg)				
	FA (sand)	CA (granite)	OPC	Water	FA (WCT)
C-WCT0	16	25.6	9	4	0
C-WCT5	15.2	25.6	9	4	0.8
C-WCT10	14.4	25.6	9	4	1.6
C-WCT15	13.6	25.6	9	4	2.4
C-WCT20	12.8	25.6	9	4	3.2
C-WCT25	12	25.6	9	4	4

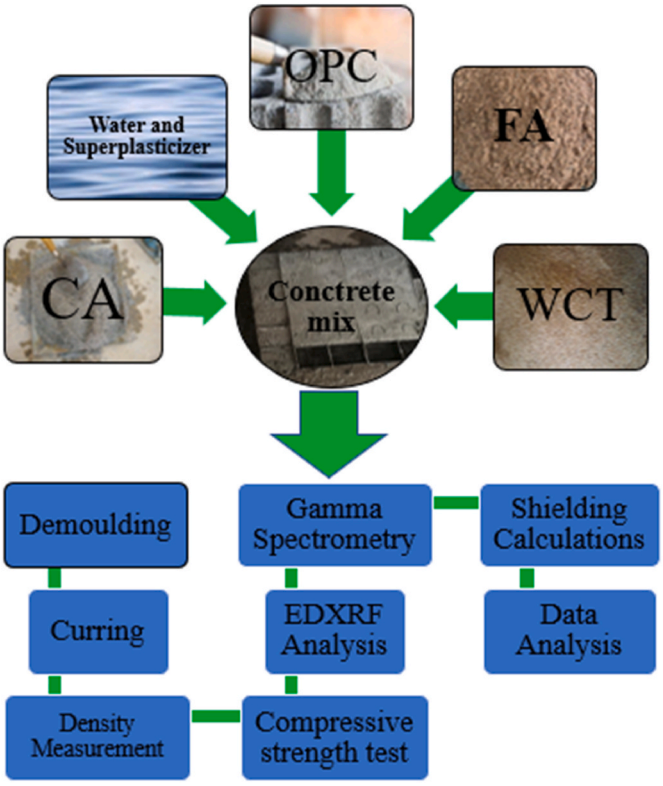


Fig. 1. Summary of the concrete preparation and analysis processes.

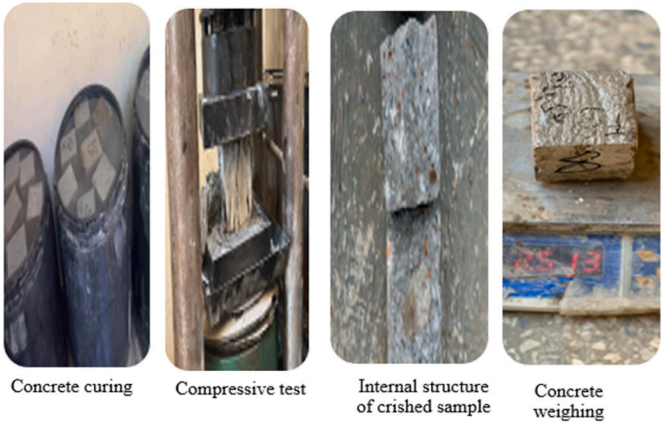


Fig. 2. Images of the curing process, compressive test measurement, internal structure of a concrete sample, and mass measurement method.

2.3. Chemical composition of concrete samples

Energy dispersive X-ray fluorescence (EDXRF) spectrometric analysis was used to examine the chemical content of the WCT and each of the formed concrete sample in order to ascertain the impact of partially substituting sand with WCT. After being sun-dried, the concrete samples were weighed repeatedly until they reached a constant weight after ten days to ensure absence of water molecules in the sample. About 20 g of pulverized moisture-free samples were combined with a binder (PVC dissolved in toluene), and placed in a hydraulic press under 20 tons of pressure to form circular pellets of 30 ± 0.1 mm. For the chemical analysis of the principal oxides in the pellets, a PANanalytical Minipal4 model PW4025/45B EDXRF spectrometer was used.

2.4. Gamma spectrometric analysis of natural radioisotopes

The gamma spectrometric method was used to determine the precise activity of the NORMS (^{238}U, ^{232}Th, and ^{40}K) in the concrete block samples using a Canberra high-purity germanium (HpGe) detector. The Genie 2000 software was used to collect and analyse the accumulated gamma-ray spectra. The details of the gamma spectrometric procedure have been discussed in previous articles (Atipo et al., 2020; Olarinoye et al., 2023).

To determine the activity of the radionuclides, Equation (1) was used (Olarinoye et al., 2023).

$$A_i = \frac{C_n}{E_\gamma M_s I_\gamma} \tag{1}$$

where A_i is the activity concentration in Bq/Kg of ^{235}U, ^{232}Th and ^{40}K in the concrete cubes, C_n is the net count per unit time observed under corresponding photo-peak, E_γ is the detector efficiency observed at a desired energy, M_s is the mass of the sample while I_γ is the gamma rays line spectrum intensity.

2.5. Calculation of radiological dose and its indices

The Absorbed dose rate ($\dot{D}$) in air owing to the activity concentration of ^{235}U, ^{232}Th and ^{40}K concentrations in the concrete cubes was obtained using Equation (2).

$$\dot{D}(nGyh^{-1}) = \sum_{i=1}^{3} A_i C_i \tag{2}$$

where A_i is the activity concentrations in Bq/Kg of ^{235}U, ^{232}Th and ^{40}K in the cubes. C_i is the dose conversion factor having the values 0.462, 0.604 and 0.0417 nGyh^{-1} per Bq/Kg for ^{235}U, ^{232}Th and ^{40}K respectively.

The annual effective dose rate (indoor) received by an occupant of a room constructed from the concrete cubes was obtained with Equation (3) (Olarinoye et al., 2023).

$$AEDR_{in}\left(\frac{mSv}{y}\right) = \dot{D}\left(\frac{nGy}{h}\right) \times 8760\left(\frac{h}{y}\right) \times 0.8 \times 0.7 \times 10^{-6}\left(\frac{mSv}{nGy}\right) \tag{3}$$

The activity concentration index I_γ is used to ascertain the radiological safety index of materials used for building. It was computed using Equation (4) (Atipo et al., 2020).

$$I = \frac{C_U}{300\left(\frac{Bq}{Kg}\right)} + \frac{C_{Th}}{200\left(\frac{Bq}{Kg}\right)} + \frac{C_K}{3000\left(\frac{Bq}{Kg}\right)} \tag{4}$$

2.6. Calculation of radiation shielding parameters

To estimate the ability of the concrete to attenuate a beam of gamma radiation and fast neutrons, the mass attenuation coefficient (μ_m) and fast neutron removal cross-section (Σ_R) were used, respectively. The μ_m of the ceramic infused concrete blocks were calculated (along with relevant photon shielding parameters such as the half-value layer, effective atomic number and photon buildup factors) using the EPICS2017 photon cross-section library (Omer et al., 2024).

The Σ_R was computed according to the standard expression (Elsheikh, 2020; Olarinoye & Oche, 2021; Piotrowski, 2021a; Rammah et al., 2021):

$$\Sigma_R = \rho \sum w_i \left(\frac{\Sigma_R}{\rho}\right)_i \tag{5}$$

where, ρ, w_i, and $\left(\frac{\Sigma_R}{\rho}\right)_i$ is the mass density of the concrete, weight fraction, and fast neutron mass removal cross section of the ith element in the sample. $\frac{\Sigma_R}{\rho}$ for each element was estimated as (Rammah et al., 2021):

$$\frac{\Sigma_R}{\rho} = 0.19Z^{-0.743} \quad \text{for } Z \leq 8; \tag{6}$$

$$\frac{\Sigma_R}{\rho} = 0.125Z^{-0.565} \quad \text{for } Z > 8 \tag{7}$$

3. Results and discussion

3.1. Compressive strength and density of concrete

The compressive strength (CS) is a crucial property that is closely linked to other mechanical attributes such as flexural strength, tensile strength, as well as the durability of concrete. The values of the CS of the prepared concrete samples after 7, 14, and 28-day curing period are presented in Fig. 3. These values represent the mean of the CS from three cubes of similar concrete species. The CS had values between 5.39 and 12.0 N/mm^2 for C-WCT0, 6.49–12.43 N/mm^2 for C-WCT5, 6.63–12.69 N/mm^2 for C-WCT10, 6.73–13.09 N/mm^2 for C-WCT15, 6.41–12.36 N/mm^2 for C-WCT20, and 6.29–12.08 N/mm^2 for C-WCT25. Generally, the CS increased as the curing age increases. This shows that age of curing improved the bonding, strength and durability of the concrete. The increase of CS is attributed to the consistent formation of product of hydration as age of curing increases (Atoyebi et al., 2020; Odeyemi et al., 2021). The increment of the CS can be modelled into a logarithmic equation with of the form:

$$CS = Aln(P) - B; \text{ for } 0.811 \leq R^2 \leq 0.9815 \tag{8}$$

where, A and B are constants whose values depend on the WCT dosage and P the curing period (days). This equation enables us to project the CS of the concrete samples for longer curing periods. The value of A and B for C-WCT0 is 4.9124 and 3.8874, respectively. For the WCT-doped concrete samples, the fitting of the coefficients (A and B) with respect to WCT dosage (x) reveals polynomial equation:

$$A = -0.0026x^2 + 0.072x + 3.976; \; R^2 = 0.7209 \tag{9}$$

$$B = -0.0016x^2 + 0.0698x + 0.8688; \; R^2 = 0.8349 \tag{10}$$

The substitution of sand with pulverized WCT up to 15% improved the CS of the prepared concrete. Hence, C-WCT15 has the highest CS values which represent about 24.9%, 19.0% and 7.3% increase after 7-,

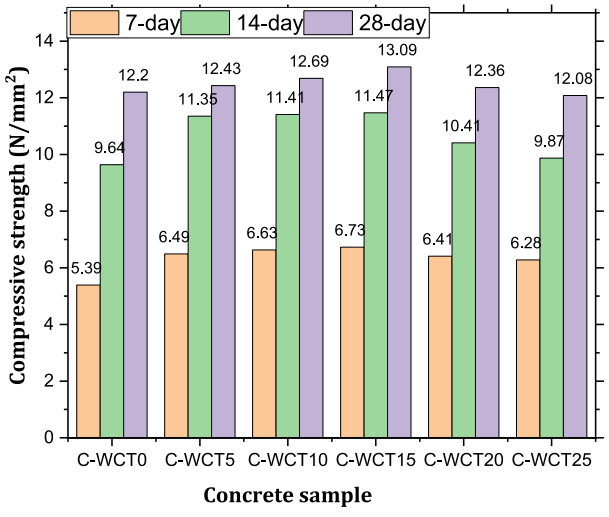


Fig. 3. Compressive strength of concrete samples at 7-, 14-, and 28-day curing periods.

14-, and 28-days curing period, respectively, compared to C-WCT0. Beyond a dosage of 15% WCT, the CS of the concrete samples begin to decline in value. This suggest that the improved bonding and the alkali-silicate reaction of the concrete components saturates and optimised at this dosage. Therefore, increasing the WCT content higher compromised the CS. In addition, the decline in the CS could be explained from the perspective of increment in surface area of the fine aggregate occasioned by the increase in the WCT content. The increase in the surface area inhibits the formation of cement gel matrix, thus, deteriorating the bonding process of the concrete matrix (Bhardwaj et al., 2023b).

The average bulk density of the concrete also exhibits a similar dependence on the WCT content as with CS. The trend of the density variation is displayed in Fig. 4. The density of the concrete varied from 2213 kg/m^3 to 2488 kg/m^3 as the WCT replaced sand from 0 to 15%. Afterwards the density decreased to 2396 kg/m^3 as the sand replacement level grows to 25%. Usually, the density of normal concrete ranges from 2200 kg/m^3 – 2600 kg/m^3 (Guerra et al., 2009; Neville et al., 2010; Opara et al., 2018). The concrete samples prepared in this study can thus be categorized as normal weight concrete. Fig. 4 shows that as the WCT dosage increases from 0 to 15%, the concrete density rose from 2213 to 2488 kg/m^3; an indication of increase in compactness. Beyond the 15% WCT dosage, the density value decreases to 2396 kg/m^3 for C-WCT25.

Clearly, the concrete sample having 15% of its fine aggregate component replace by WCT have the best mechanical attribute. This is in consonance with an earlier study (Mustafy et al., 2022) that concluded that concrete samples prepared with recycled waste ceramics as fine aggregate had the capacity to improve CS.

3.2. Chemical content of concrete

The major oxides contained in the WCT and concrete samples are given in Table 2. The table clearly shows that SiO_2 and CaO are the major oxides in the concrete sample. Both oxides make up more than 80% by weight of the chemical oxides in the WCT and concrete. The introduction of the WCT perturbed the chemical composition of undoped concrete as presented in Table 2. The oxides of Al, Ca, Fe, K, and Si constitute more than 95% of the chemical content of the undoped concrete sample (CWCT0). The introduction of WCT perturbed the chemical composition of the concrete. The concentration of SiO_2 increases while that of CaO decreases when WCT was added to the concrete in C-WCR5 as expected based on the chemical composition of WCT. Increasing the WCT content change the chemical content in different ways. The introduction of WCT improved the silicate content of the concrete samples and decreased the amount of CaO. The higher SiO_2 content of WCT could increase the alkali-silicate reaction in the concrete. This often leads to lower concrete strength, increase cracks, and decreases durability (Figueira et al., 2019; Pan et al., 2012). On the other hand, the relatively lower SiO_2/CaO ratio of WCT compared to C-WCT0 showed that WCT could be used to improve the compressive strength of the concrete, since lower CaO and higher SiO_2 concentrations in concrete improves mechanical strength (Abdalla et al., 2022; Jaf et al., 2023). Therefore, a balance in the sand to WCT ratio is required to optimise the mechanical and other properties of concrete.

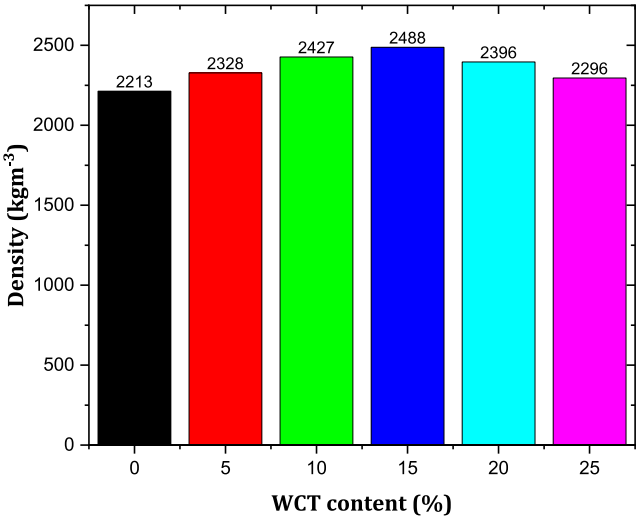


Fig. 4. Concrete density for different WCT dosage.

3.3. Activity concentration

The activity concentrations of ^{238}U, ^{232}Th, and ^{40}K in the concrete samples are presented in Table 3. The result shows that the concentration of ^{238}U ranged from 12.25 to 24.48 Bq/kg, with a mean value of 19.53 Bq/kg. Similarly, the range (and mean) of the specific activities of ^{232}Th and ^{40}K, respectively, are: 90.78–146.37 (with a mean of 104.07 Bq/kg) and 567.94–987.71 Bq/kg (with a mean of 659.39 Bq/kg). The radionuclide concentrations in the concret samples are observed to follow the trend $C_k > C_{Th} > C_{U,}$ which is consistent with the trend of the natural abundance of radioactive atoms in uncontaminated soils (Olarinoye et al., 2023). Except for ^{238}U, the mean activities of ^{232}Th and ^{40}K were above the global mean values of 30, 35, and 400Bq/kg (Gaspar et al., 2021; Olarinoye et al., 2023). The data in Table 3 also reveals that the activity concentration of ^{232}Th and ^{40}K in the control specimen (C-WCT0) is higher compared to other samples with varying degrees of sand replacement. This simply shows that the river sand used for the concrete had a higher ^{232}Th and ^{40}K contents than the WCT. The WCT tiles thus lowered the specific activities of the two NORMs in the concrete. The values of C_{Th} increased gradually with the replacement percentage but never got to the peak value of the control (C-WCT0). For C_K, its value increases as the replacement level grew up to 10% and subsequently decreases with additional replacement level. This, however, was not the case for C_U, as its value kept increasing with an increase in the WCT. Furthermore, the radiological content of the concrete cubes is compared with other concrete blocks from within Nigeria, Ghana, and Finland, as shown in Table 4. When compared with previous studies, the ^{238}U, ^{232}Th, and ^{40}K mean activity concentrations found in the concrete cubes in this study were 1.99, 5.08, and 6.16 times, respectively, greater than the value found by Otoo et al. in 2018 (Otoo et al., 2018) in the greater Accra region of Ghana. However, the activity concentrations were found to be lower than those obtained by Olarinoye et al. in 2023 (Olarinoye et al., 2023). The specific activity of ^{232}Th was higher compared to a study in Finland (Smetsers & Tomas, 2019), while that of ^{40}K was higher for all sampled studies except those from Finland. The variations in the radionuclide concentrations are basically predicated on the variations in the sources (parent rocks) from which the cement and aggregates of the concrete were derived. For example, the fine aggregates used by Olarinoye et al. in 2023 (Olarinoye et al., 2023) were mine waste (tailings), which had earlier been shown to possess elevated NORM concentrations. Therefore, giving the concrete produced the tailings elevated NORM concentration. To control the indoor radiation dose level, it is essential to screen building materials such as cements and aggregates for their MORM content.

3.4. Radiological dose parameters

The absorbed dose rate, annual effective dose, and gamma dose index were obtained using Equations (2)–(4), respectively, and the obtained values are presented in Table 5. The absorbed dose ranged from 90.149 to 135.255 nGy/h, with a mean value of 100.02 nGy/h. The mean value obtained is 2.22 and 1.19 times greater than the outdoor and indoor exposure world averages, respectively (UNSCEAR (United Nations Scientific Committee on the Effects of Atomic Radiation) and Sources and Effects of Ionizing Radiation, 2000). Thus, as a result of the above, a mean indoor AEDE of 0.491 mSv/y was obtained. All the cubes

Table 2
Major oxides in the prepared concrete samples.

Major oxides		Concrete sample					
	WCT	C-WCT0	C-WCT5	C-WCT10	C-WCT15	C-WCT20	C-WCT25
MgO	0	0.697	0.684	0.684	0.685	0.685	0.685
Al_2O_3	19.752	7.111	7.266	7.578	7.89	8.203	8.515
SiO_2	47.975	31.408	39.317	38.459	37.602	36.745	35.887
P_2O_5	0.082	0	0.001	0.003	0.005	0.007	0.009
SO_3	0.791	1.143	1.005	1.018	1.031	1.045	1.058
K_2O	1.309	2.628	2.597	2.567	2.536	2.506	2.476
CaO	18.879	49.864	42.604	42.969	43.334	43.7	44.065
TiO_2	2.644	0.507	0.534	0.587	0.639	0.692	0.744
V_2O_5	0.114	0.017	0.02	0.022	0.024	0.026	0.028
Cr_2O_3	0.057	0.074	0.074	0.074	0.073	0.072	0.072
MnO	0.076	0.111	0.102	0.102	0.103	0.103	0.104
Fe_2O_3	6.413	4.819	4.347	4.467	4.587	4.707	4.827
Co_2O_3	0.032	0.028	0.026	0.026	0.027	0.027	0.027
NiO	0.006	0.004	0.003	0.003	0.004	0.004	0.004
CuO	0.056	0.051	0.05	0.05	0.051	0.051	0.051
ZnO	0.09	0.008	0.009	0.011	0.013	0.015	0.017
SrO	0.099	0.478	0.408	0.409	0.41	0.412	0.413
ZrO_2	0.77	0.035	0.049	0.066	0.083	0.101	0.118
Nb_2O_3	0.02	0.012	0.011	0.011	0.011	0.012	0.012
MoO_3	0.008	0.014	0.012	0.012	0.012	0.012	0.012
Ag_2O	0.029	0.041	0.037	0.037	0.037	0.038	0.038
SnO_2	0.038	0.591	0.495	0.496	0.497	0.498	0.499
BaO	0.085	0.318	0.297	0.294	0.291	0.288	0.285
Ta_2O_5	0.041	0.041	0.04	0.04	0.04	0.04	0.04
Density (kg/m^3)	2413	2213	2328	2426	2488	2396	2296

Table 3
Mean specific activities of NORMs in the concrete samples.

Concrete sample	Activity concentration (Bq/kg)		
	^{238}U	^{232}Th	^{40}K
C-WCT0	12.25 ± 2.63	146.37 ± 23.52	987.71 ± 27.13
C-WCT5	17.12 ± 2.35	90.78 ± 12.67	657.28 ± 32.78
C-WCT10	17.94 ± 4.22	92.21 ± 10.22	652.52 ± 22.89
C-WCT15	21.78 ± 3.68	96.61 ± 11.65	567.94 ± 34.28
C-WCT20	23.63 ± 4.98	99.02 ± 15.39	583.35 ± 12.90
C-WCT25	24.48 ± 6.54	99.43 ± 12.36	599.76 ± 22.61
Minimum	12.25	90.78	562.52
Maximum	24.47	146.37	985.7
Mean	19.53	104.07	659.39

Table 4
Comparison of specific activity of concrete blocks from different studies.

Location	Specific Activity (Bq/kg)			Ref.
	^{238}U	^{232}Th	^{40}K	
Ghana	9.80	20.50	107.00	Otoo et al. (2018)
Nigeria	29.00	26.00	289.00	Ademola and Oguneletu (2005)
Nigeria	120.00	248.31	635.10	Olarinoye et al. (2023)
Finland	33.30	34.00	800.00	Smetsers and Tomas (2019)
Nigeria	19.53	104.07	659.39	This study

Table 5
Mean specific activities of NORMs and Dose parameters in the concrete samples.

Concrete sample	Mean activity (Bq/kg)			Dose parameters		
	^{238}U	^{232}Th	^{40}K	D (nGy/h)	AEDE (mSv/y)	Iγ
C-WCT0	12.25	146.37	987.71	135.255	0.663	1.1
C-WCT5	17.12	90.78	657.28	90.149	0.442	0.7
C-WCT10	17.94	92.21	652.52	91.193	0.447	0.7
C-WCT15	21.78	96.61	567.94	92.097	0.451	0.7
C-WCT20	23.63	99.02	583.35	95.05	0.466	0.7
C-WCT25	24.48	99.43	599.76	96.375	0.472	0.7
Mean	19.53	104.07	659.39	100.02	0.491	0.81

had AEDE values slightly above the 0.41 mSv/y world average. It is also pertinent to note that the AEDE of the control sample is about 1.35 times the average value for all the samples under study. This further emphasises the influence of the WCT in lowering the radiation dose burden on residents of buildings constructed from WCT-doped concrete.

The activity concentration index I_g is used for studying materials with the propensity to exceed referenced dose limits. To ensure this doesn't happen, the value of I_g must be less than or equal to unity (i.e., $I_g \leq 1$). The range of I as reported in Table 5 is 0.7–1.1. The value of I_g is used to ascertain what material or how much of a material can be used for a building. For $I_g \geq 1$, the material is used only superficially (Olarinoye et al., 2023), while for $I_g \leq 1$, the material can be used as desired. This simply means that the control sample C-WCT0 is unfit for bulk usage, as more exposure could result from making a large mass of concrete with it. However, the introduction of WCT reduced the gamma index and makes the concrete samples containing WCT useful in bulk volume for building. The introduction of WCT into the concrete matrix thus made the concrete radiologically safer as a building material or as a biological shield.

3.5. Indoor gamma dose within a standard room

In order to assess the radiological dose implications of using the prepared concrete samples as building materials further, the indoor gamma dose rate at the centre of a standard room (of dimensions 5 × 4 × 2.8 m^3) is evaluated based on the expression (Olarinoye et al., 2023):

$$\dot{D} = \frac{\pi \Gamma A_m \rho}{\mu_c} ln\left(\frac{H^2 + R^2}{H^2}\right).\left(2\left(1 - e^{-\mu_c T}\right) - \mu_c T e^{-\mu_c T}\right) \quad (11)$$

where, μ_c is the linear attenuation coefficient of the concrete wall at different gamma energies emitted by the three NORMs, A_m, ρ, and Γ, is the specific activity of the radionuclides, density of the concrete used for constructing the room walls, and the specific gamma constant of the NORMs. Based on a model concrete walls, floor, and roof of thickness 20 cm and density 2.34 g/cm^3, the indoor dose rates were estimated, and the values are displayed in Table 6. This model gives the maximum possible indoor dose rates provided other materials to be used in the construction of floors and roofs have lower specific activities and the

Table 6
Indoor dose parameters at the centre. of 5 cm × 4 cm X 2.5 cm room.

Concrete Sample	Dose Parameters	
	D (nGy/h)	AEDR (mSv/y)
C-WCT0	233.42	1.15
C-WCT5	156.18	0.77
C-WCT10	157.89	0.77
C-WCT15	158.62	0.78
C-WCT20	163.75	0.80
C-WCT25	166.17	0.82
Mean	171.44	0.84

outdoor background dose rate is lower compared to the concrete samples. The estimated absorbed dose rate ranged from 156.18 to 233.42 nGy/h with a mean value of 171.44 nGy/h. In addition, the AEDR ranged from 0.80 to 1.15 mSv/y. The maximum and minimum values of both parameters were obtained for C-WCT0 and C-WCT10, respectively. While there was a thin line between the values of the dose indices for C-WCT10 and C-WCT15. Based on the values of the AEDR, the total dose contributions of the walls at the centre of the standard room are less than the 1 mSv/y recommended dose limits for public exposures. The absorbed dose rate obtained in this model could be lower in practical situations as other materials with lower specific activities are used for the construction of the roof and floors of the room. The presence of doors and windows as obtainable in practicable situations would further decrease the indoor dose burdens from the concrete samples. Consequently, the prepared concrete samples are radiologically safe and could be used as building materials in bulk. Also, the influence of the WCT on the dose burden of the room is quite evident in Table 6. This affirms that using alternative materials with lower specific activity to replace sand is radiologically desirable in the construction of concrete.

3.6. Radiation shielding parameters

Concrete is a common and cheaper material for radiation shielding worldwide. Consequently, determining the shielding parameters is one of the basic characterizations of concrete samples. In this research, we concentrate on the parameters related to gamma-rays and neutron absorption. These two radiation types are mostly adopted in nuclear facilities. In addition, they are highly penetrating and produced as secondary radiation in the interaction of other radiation types with matter. The mass attenuation coefficients (MACs) of the concrete were computed using the EPICS2017 photon cross-section library for standard photon energy sources. The obtained MACs and LACS are plotted against gamma photon energy, as displayed in Figs. 5 and 6. The figures show a strong photon energy dependence exists for both attenuation parameters, and the variation patterns are similar for all concrete samples. Generally, high values of attenuation coefficients were recorded at the least energy (59.54 keV) and the minimum at 1.3 MeV. The decline in the values of the attenuation coefficients was initially rapid and later became less intense. The MACs of the concrete ranged from 0.612 to 0.054 cm^2/g for C-WCT0, 0.572–0.055 cm^2/g for C-WCT5, 0.574–0.055 cm^2/g for C-WCT10, 0.576–0.055 cm^2/g for C-WCT15, 0.578–0.054 cm^2/g for C-WCT20, and 0.0580–0.054 cm^2/g for C-WCT25. The variations in the values of the attenuation coefficient can be attributed to the energy and chemical composition dependences of the photon interaction processes. The continued decline in the values of MAC is an indication of lower absorption competence as energy increases. This means that the interaction cross-sections are lower at higher photon energies. In theory, there are three interaction processes namely, pair production absorption (PPA), incoherent scattering (ICS), and photoelectric absorption (PEA), with cross-sections denoted as τ, σ, and κ with approximate photon energy (E_{ph}) and chemical content (Z) relations (Gharam et al., 2023):

$$\sigma \propto Z^5 E_{ph}^{-3.5} \quad (12)$$

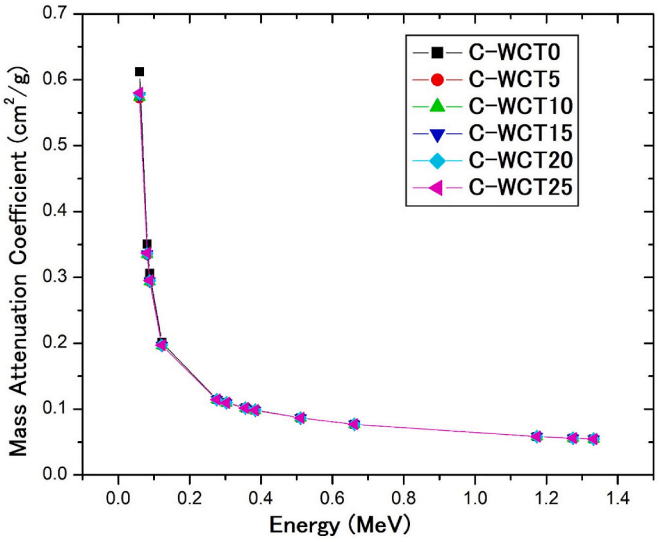


Fig. 5. Variation of Mass Attenuation Coefficient of concrete samples with energy.

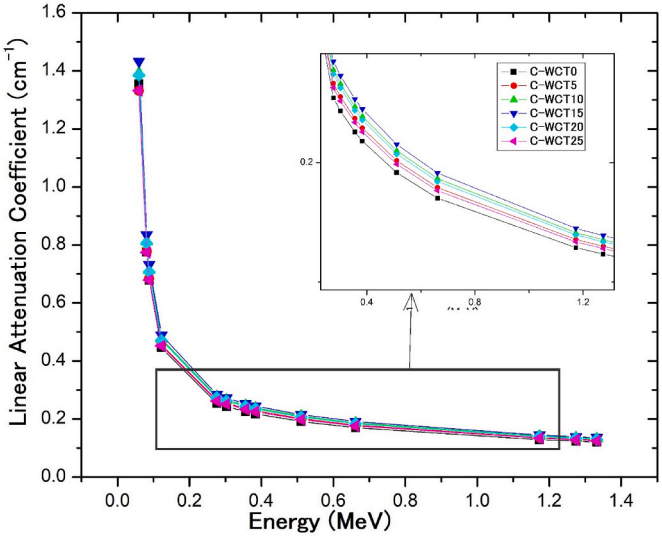


Fig. 6. Variation of Linear Attenuation Coefficient of concrete with energy.

$$\tau \propto Z E_{ph}^{-1} \quad (13)$$

$$\kappa \propto Z^2 (ln\, E_{ph})^{0.5} \quad (14)$$

The photoelectric absorption process is the dominant interaction at low energy. The high but rapidly declining MAC values at the lower end of the energy range are attributed to the relationship between σ and photon energy. In addition, the continuous decrement suggests the contribution of PPA to the MAC is minimal. Furthermore, the LACs were between 0.1207 and 1.3539 cm^{-1}, 0.1271 and 1.3307 cm^{-1}, 0.1324 and 1.3917 cm^{-1}, 0.1358 and 1.4323 cm^{-1}, 0.1307 and 1.3849 cm^{-1}, and 0.1252 and 1.3317 cm^{-1} for C-WCT 0–25. At each energy, the LACs of the concrete trend are in the order C-WCT15 > C-WCT10 > C-WCT20 > C-WCT5 > C-WCT25 > C-WCT0, as seen in Fig. 6. This trend is consistent with the density of the concrete samples.

The half-value (HVL) is an important quantity in radiation shielding analysis. It is the thickness of a barrier that is capable of reducing photon flux by half of its incident level. It is thus a simple and practical parameter for assessing the shielding performance of a medium.

Theoretically, it is inversely proportional to LAC; hence, the higher the HVL, the more efficient a material is at photon attenuation. In Fig. 7, the HVL of C-WCT15 is qualitatively compared with that of traditional shielding materials, namely, ordinary concrete (OC) (Bashter, 1997), barite concrete (Bashter, 1997), and commercial glass shield (RS 253 G18) (Speid, 1991) at four photon energies (15 keV, 100 keV, 1 MeV, and 10 MeV). The figure shows that C-WCT15 concrete has a better photon absorption capacity at all the energies considered compared to OC. However, the BC is better than C-WCT15 at low energies (15 keV and 100 keV), but at higher energies, its shielding ability is comparable to that of the ceramic-doped concrete. With respect to commercial SCHOTT glass (RS 253 G18), C-WCT15 is an inferior absorber at 15 keV. However, the ceramic-doped concrete can outshine the glass at higher energies due to its lower HVLs. The variations in the shielding abilities of the different materials can be attributed to their different chemical compositions. BC contains dense aggregates having high atomic number elements, such as Ba; it is thus denser and less transparent to photons compared to the other materials in the figure. The C-WCT15 concrete contains regular aggregates and is lead-free, unlike the SCHOTT glass. This makes it more attractive from an environmental health perspective. To improve the shielding competence of C-WCT15 concrete, dense aggregates can be used. In addition, the thickness of the concrete can be increased to improve its gamma radiation shielding competence. It is clear from the aforementioned comparison that concrete made from waste ceramic can be used as an effective shielding concrete.

The fast neutron removal cross section was computed in order to ascertain the fast neutron moderation capacity of the glasses. The computed Σ_R values are 0.0682, 0.0729, 0.0759, 0.0777, 0.0748 and 0.0716 cm^{-1} for C-WCT0, C-WCT5, C-WCT10, C-WCT15, C-WCT20, and C-WCT25, respectively. The growth in the moderation capacity of the concrete samples is displayed in Fig. 8. The maximum value of Σ_R at C-WCT15 shows that the increase in WCT to the optimum level affects the Σ_R positively. However, when compared with OC and BC with Σ_R values of 0.093 cm^{-1} and 1.003 cm^{-1} (Piotrowski, 2021b), respectively, the waste ceramic-doped concrete samples possess lower fast neutron moderation capacity.

4. Conclusion

The influence of replacing fine aggregate with fine waste ceramic tiles on the physical, mechanical, and radiological attributes of normal-strength concrete was investigated in this study. Six concrete samples coded as C-WCT0, C-WCT5, C-WCT10, C-WCT15, C-WCT20, and C-WCT25, representing concrete samples in which the sand component was replaced by 0, 5, 10, 15, 20, and 25%, respectively, were successfully prepared. The values of the CS of the prepared concrete samples after 7, 14, and 28-day curing periods had values between 5.39 and 12.0 N/mm^2 for C-WCT0, 6.49 and 12.43 N/mm2 for C-WCT5, 6.63 and 12.69 N/mm2 for C-WCT10, 6.73 and 13.09 N/mm^2 for C-WCT15, 6.41 and 12.36 N/mm^2 for C-WCT20, and 6.29 and 12.08 N/mm^2 for C-WCT25. The substitution of sand with pulverized WCT improved the CS of the prepared concrete by up to 15%. As the WCT dosage increased from 0 to 15%, the concrete density rose from 2213 to 2488 kg/m^3; an indication of an increase in compactness. Beyond the 15% WCT dosage, the density value decreases to 2396 kg/m^3 for C-WCT25. The radionuclide concentrations in the waste ceramic-doped concrete followed the trend $C_K > C_{Th} > C_U$ which is a trend of the natural abundance of radioactive atoms noticeable in uncontaminated soils. The introduction of WCT into the concrete matrix made the concrete radiologically safer as a building material or as a biological shield. The optimum WCT content as fine aggregate replacement in concrete preparation that gives the highest CS and photon shielding effectiveness is 15%. The MACs of the concrete ranged from 0.612 to 0.054 cm^2/g for C-WCT0, 0.572–0.055 cm^2/g for C-WCT5, 0.574–0.055 cm^2/g for C-WCT10, 0.576–0.055 cm^2/g for C-WCT15, 0.578–0.054 cm^2/g for C-WCT20, and 0.0580–0.054 cm^2/g for C-WCT25. The C-WCT15 had shielding abilities comparable to conventional shielding materials. The use of WCT as aggregate in concrete production is a sustainable and environmental-friendly way of producing concrete for general civil engineering and shielding applications in medical and other radiation facilities. This study also affirms that using alternative materials with lower specific activity to replace sand is radiologically desirable in reducing the indoor radiation dose of occupants of concrete-based structures. The WCT-based concrete is stronger, radiologically safer, and more effective radiation absorber. Although this study showed that the use of waste ceramic tiles as replacement for sand in concrete making is advantageous from waste recycling, resource management, and radiological safety perspectives, it is however limited in terms of other concrete properties. The stability and radiation-induced activation process in radiation environment was not investigated, hence the long-term use of the concrete as radiation shield could not be verified. In addition, the thermal, electrical, and chemical durability of the investigated concrete needs to be probed in order to know the stability and environmental factors that could influence the concrete behaviour. Based on the results from this study, replacing 15% sand with waste ceramic tiles of the same particles size enhanced the compressive strength, density, radiation

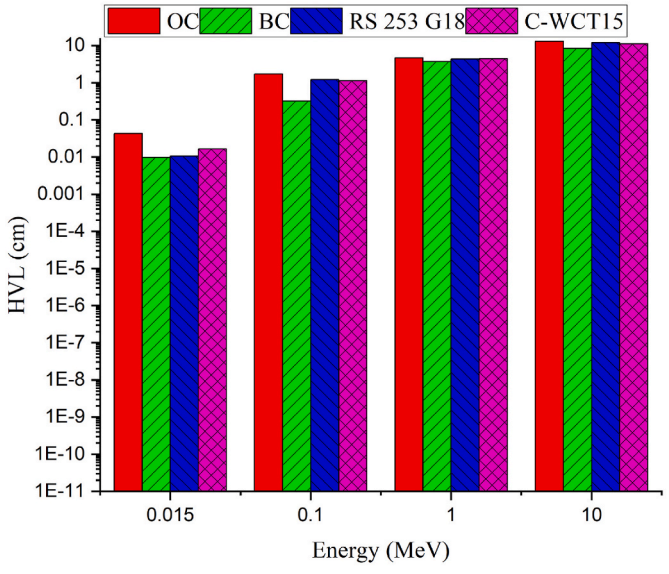


Fig. 7. Comparison between photon absorption capacity of C-WCT15 and traditional shielding materials.

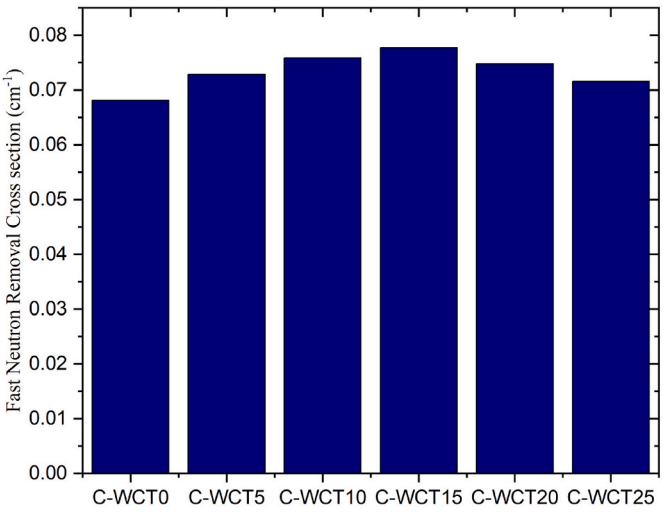


Fig. 8. Fast neutron removal cross section obtained using PHY-X and FTNCS.

shielding and safety features of concrete.

CRediT authorship contribution statement

I.O. Olarinoye: Writing - Original Draft. **M.T. Kolo:** Methodology and Experimental work. **D.B. Amuda:** Methodology and Experimental work. **C.O. Oche:** Methodology and Experimental work. **B. Mohammed:** Methodology and Experimental work. **Jamila S. Alzahrani:** Supervision and Project administration. **M. S. Al-Buriahi:** Review & Editing.

Acknowledgement

The authors express their gratitude to Princess Nourah bint Abdulrahman University Researchers Supporting Project number (PNURSP 2024R48), Princess Nourah bint Abdulrahman University, Riyadh, Saudi Arabia.

References

Abdalla, A. A., & Salih Mohammed, A. (2022). Theoretical models to evaluate the effect of SiO2 and CaO contents on the long-term compressive strength of cement mortar modified with cement kiln dust (CKD). *Archives of Civil and Mechanical Engineering, 22*(3), 105.

Ademola, J. A., & Oguneletu, P. O. (2005). Radionuclide content of concrete building blocks and radiation dose rates in some dwellings in Ibadan, Nigeria. *Journal of Environmental Radioactivity, 81*(1), 107–113.

Ahmadi, M., Farzin, S., Hassani, A., & Motamedi, M. (2017). Mechanical properties of the concrete containing recycled fibers and aggregates. *Construction and Building Materials, 144*, 392–398.

Al-Buriahi, M. S., Alrowaili, Z. A., Alsufyani, S. J., Olarinoye, I. O., Alharbi, A. N., Sriwunkum, C., & Kebaili, I. (2022). The role of PbF2 on the gamma-ray photon, charged particles, and neutron shielding prowess of novel lead fluoro bismuth borate glasses. *Journal of Materials Science: Materials in Electronics, 33*(3), 1123–1139.

Al-Buriahi, M. S., Gaikwad, D. K., Hegazy, H. H., Sriwunkum, C., & Neffati, R. (2021). Fe-based alloys and their shielding properties against directly and indirectly ionizing radiation by using FLUKA simulations. *Physica Scripta, 96*(4), Article 045303.

Al-Manaseer, A. A., & Dalal, T. R. (1997). Concrete containing plastic aggregates. *Concrete International, 19*(8), 47–52.

Alalawi, A., Al-Buriahi, M. S., Sayyed, M. I., Akyildirim, H., Arslan, H., Zaid, M. H. M., & Tonguç, B. T. (2020). Influence of lead and zinc oxides on the radiation shielding properties of tellurite glass systems. *Ceramics International, 46*(11), 17300–17306.

Ali, B., Fahad, M., Mohammed, A. S., Ahmed, H., Elhag, A. B., & Azab, M. (2022). Improving the performance of recycled aggregate concrete using nylon waste fibers. *Case Studies in Construction Materials, 17*, Article e01468.

Alzahrani, J. S., Alrowaili, Z. A., Eke, C., Mahmoud, Z. M., Mutuwong, C., & Al-Buriahi, M. S. (2022). Nuclear shielding properties of Ni-, Fe-, Pb-, and W-based alloys. *Radiation Physics and Chemistry, 195*, Article 110090.

ASTM C 109/C 109M – 08. (2008). *Standard test method for compressive strength of hydraulic cement mortars*. West Conshohocken, PA, USA: ASTM International.

Atipo, M., Olarinoye, O., & Awojoyogbe, B. (2020). Comparative analysis of NORM concentration in mineral soils and tailings from a tin-mine in Nigeria. *Environmental Earth Sciences, 79*(16), 394.

Atoyebi, O. D., Ikubanni, P. P., Adesina, A., Araoye, O. V., & Davies, I. E. E. (2020). Effect of curing methods on the strength of interlocking paving blocks. *Cogent Engineering, 7*(1), Article 1770914.

Awoyera, P. O., Ndambuki, J. M., Akinmusuru, J. O., & Omole, D. O. (2018). Characterization of ceramic waste aggregate concrete. *HBRC journal, 14*(3), 282–287.

Bashter, I. I. (1997). Calculation of radiation attenuation coefficients for shielding concretes. *Annals of Nuclear Energy, 24*(17), 1389–1401.

Bhardwaj, A., Kumar, P., Siddique, S., & Shukla, A. (2023a). Comprehensive review on utilization of waste foundry sand in concrete. *European Journal of Environmental and Civil Engineering, 27*(3), 1056–1087.

Bhardwaj, A., Kumar, P., Siddique, S., & Shukla, A. (2023b). Comprehensive review on utilization of waste foundry sand in concrete. *European Journal of Environmental and Civil Engineering, 27*(3), 1056–1087.

Elsheikh, N. A. (2020). Gamma-ray and neutron shielding features for some fast neutron moderators of interest in 252Cf-based boron neutron capture therapy. *Applied Radiation and Isotopes, 156*, Article 109012.

Figueira, R. B., Sousa, R., Coelho, L., Azenha, M., De Almeida, J. M., Jorge, P. A. S., & Silva, C. J. R. (2019). Alkali-silica reaction in concrete: Mechanisms, mitigation and test methods. *Construction and Building Materials, 222*, 903–931.

Fritts, R. (2019). The world needs to get serious about managing sand, UN report says. *Science*. https://www.sciencemag.org/news/2019/05/world-needs-get-serious-about-managing-sand-says-un-report.

Gaspar, L., Lizaga, I., & Navas, A. (2021). Spatial distribution of fallout and lithogenic radionuclides controlled by soil carbon and water erosion in an agroforestry South-Pyrenean catchment. *Geoderma, 391*, Article 114941.

Gharam, A. A., Alrowaili, Z. A., Eke, C., Boukhris, I., Olarinoye, I. O., Alzahrani, J. S., Sriwunkum, C., & Al-Buriahi, M. S. (2023). Charged and uncharged radiation shielding performance of CaO+ZnO+Na2B2O7 glass system. *Radiation Physics and Chemistry, 205*, Article 110673, 2023.

Guerra, I., Vivar, I., Llamas, B., Juan, A., & Moran, J. (2009). Eco-efficient concretes: The effects of using recycled ceramic material from sanitary installations on the mechanical properties of concrete. *Waste management, 29*(2), 643–646.

Ibrahim, A. K., Dhahir, H. Y., Mohammed, A. S., Omar, H. A., & Sedo, A. H. (2023). The effectiveness of surrogate models in predicting the long-term behavior of varying compressive strength ranges of recycled concrete aggregate for a variety of shapes and sizes of specimens. *Archives of Civil and Mechanical Engineering, 23*(1), 61.

Ismail, Z. Z., & Al-Hashmi, E. A. (2008). Use of waste plastic in concrete mixture as aggregate replacement. *Waste manage*ment, 28*(11), 2041–2047.

Jaf, D. K. I., Abdulrahman, A. S., Abdulrahman, P. I., Mohammed, A. S., Kurda, R., Ahmed, H. U., & Faraj, R. H. (2023). Effitioned soft computing models to evaluate the impact of silicon dioxide (SiO2) to calcium oxide (CaO) ratio in fly ash on the compressive strength of concrete. *Journal of Building Engineering, 74*, Article 106820.

Kanthe, V. N. (2021). Effect of superplasticizer on strength and durability of rice husk ash concrete. *Iranian (Iranica) Journal of Energy & Environment, 12*(3), 204–208.

Kaplan, G., Gulcan, A., Cagdas, B., & Bayraktar, O. Y. (2021). The impact of recycled coarse aggregates obtained from waste concretes on lightweight pervious concrete properties. *Environmental Science and Pollution Research, 28*, 17369–17394.

Khaleel, Y. U., Qubad, S. D., Mohammed, A. S., & Faraj, R. H. (2024). Reinventing concrete: A comprehensive review of mechanical strength with recycled plastic waste integration. *Journal of Building Pathology and Rehabilitation, 9*(2), 111.

Kurda, R., Silvestre, J. D., & de Brito, J. (2018). Life cycle assessment of concrete made with high volume of recycled concrete aggregates and fly ash. *Resources, Conservation and Recycling, 139*, 407–417.

Lopez, V., Llamas, B., Juan, A., Moran, J. M., & Guerra, I. (2007). Eco-efficient concretes: Impact of the use of white ceramic powder on the mechanical properties of concrete. *Biosystems Engineering, 96*(4), 559–564.

Mansour, M. A., Ismail, M. H. B., Imran Latif, Q. B. A., Alshalif, A. F., Milad, A., & Bargi, W. A. A. (2023). A systematic review of the concrete durability incorporating recycled glass. *Sustainability, 15*(4), 3568.

Mishra, R. K., Tripathi, R. K., & Dubey, V. (2016). Early age shrinkage pattern of concrete on replacement of fine aggregate with industrial by-product. *Journal of radiation research and applied sciences, 9*(4), 386–391.

Mustafy, T., Hasan, M. M., Ahmed Shuvo, N., & Sarwar Mujib, J. M. (2022). *Characterization of mechanical properties of concrete recycled ceramic and glass powder exposed to elevated temperatures*.

Neville, A. M., & Brooks, J. J. (2010). *Concrete technology* (2nd ed.). Essex, UK: Pearson Education.

Odeyemi, S. O., Abdulwahab, R., Anifowose, M. A., & Atoyebi, O. D. (2021). *Effect of curing methods on the compressive strengths of palm kernel shell concrete*.

Olarinoye, O. I., Idris, M. M., & Kure, M. (2021). Photon and fast neutron transmission parameters of metakaolin doped concrete. *Journal of Building Material Science, 3*(2), 58–66.

Olarinoye, I. O., Kolo, M. T., Shittu, H. O., & Anumah, A. S. (2023). Estimation of indoor gamma radiation dose rate from concrete blocks constructed from tin mine tailings. *Journal of Building Engineering*, Article 105934.

Olarinoye, O., & Oche, C. (2021). Gamma-ray and fast neutron shielding parameters of two new titanium-based bulk metallic glasses. *Iranian Journal of Medical Physics, 18*(2).

Olarinoye, I. O., Rammah, Y. S., Alraddadi, S., Sriwunkum, C., Abd El-Rehim, A. F., Zahran, H. Y., & Al-Buriahi, M. S. (2020). The effects of La2O3 addition on mechanical and nuclear shielding properties for zinc borate glasses using Monte Carlo simulation. *Ceramics International, 46*(18), 29191–29198.

Omer, B., Jaf, D. K. I., Abdalla, A., Mohammed, A. S., Abdulrahman, P. I., & Kurda, R. (2024). Advanced modeling for predicting compressive strength in fly ash-modified recycled aggregate concrete: XGboost, MEP, MARS, and ANN approaches. *Innovative Infrastructure Solutions, 9*(3), 61.

Opara, H. E., Eziefula, U. G., & Eziefula, B. I. (2018). Comparison of physical and mechanical properties of river sand concrete with quarry dust concrete. *Selected Scientific Papers - Journal of Civil Engineering, 13*(s1), 127–134.

Otoo, F., Darko, E. O., Garavaglia, M., Giovani, C., Pividore, S., Andam, A. B., … Adu, S. (2018). Public exposure to natural radioactivity and radon exhalation rate in construction materials used within Greater Accra Region of Ghana. *Scientific African, 1*, Article e00009.

Pan, J. W., Feng, Y. T., Wang, J. T., Sun, Q. C., Zhang, C. H., & Owen, D. R. J. (2012). Modeling of alkali-silica reaction in concrete: A review. *Frontiers of Structural and Civil Engineering, 6*, 1–18.

Piotrowski, T. (2021a). Neutron shielding evaluation of concretes and mortars: A review. *Construction and Building Materials, 277*, Article 122238.

Piotrowski, T. (2021b). Neutron shielding evaluation of concretes and mortars: A review. *Construction and Building Materials, 277*, Article 122238.

Qaidi, S. M., Atrushi, D. S., Mohammed, A. S., Ahmed, H. U., Faraj, R. H., Emad, W., … Najm, H. M. (2022). Ultra-high-performance geopolymer concrete: A review. *Construction and Building Materials, 346*, Article 128495.

Rammah, Y. S., El-Agawany, F. I., Gamal, A., Olarinoye, I. O., Ahmed, E. M., & Abouhaswa, A. S. (2021). Responsibility of Bi2O3 content in photon, alpha, proton, fast and thermal neutron shielding capacity and elastic moduli of ZnO/B2O3/Bi2O3 glasses. *Journal of Inorganic and Organometallic Polymers and Materials, 31*(8), 3505–3524.

Rentier, E. S., & Cammeraat, L. H. (2022). The environmental impacts of river sand mining. *Science of The Total Environment, 838*, Article 155877.

Saikia, N., & De Brito, J. (2014). Mechanical properties and abrasion behaviour of concrete containing shredded PET bottle waste as a partial substitution of natural aggregate. *Construction and Building Materials, 52*, 236–244.

Singh, A., Kumar, R., Mehta, P. K., & Tripathi, D. (2020). Effect of nitric acid on Rice Husk Ash steel fiber reinforced concrete. *Materials Today: Proceedings, 27*, 995–1000.

Smetsers, R. C., & Tomas, J. M. (2019). A practical approach to limit the radiation dose from building materials applied in dwellings, in compliance with the Euratom Basic Safety Standards. *Journal of Environmental Radioactivity, 196*, 40–49.

Speid, B. (1991). *Radiation-shielding glasses providing safety against electrical discharge and being resistant to discoloration.* Google Patents. https://patents.google.com/patent/US5073524A/en. (Accessed 17 September 2023).

Tayeh, B. A., Akeed, M. H., Qaidi, S., & Bakar, B. A. (2022). Influence of the proportion of materials on the rheology and mechanical strength of ultrahigh-performance concrete. *Case Studies in Construction Materials, 17*, Article e01433.

Thorneycroft, J., Orr, J., Savoikar, P., & Ball, R. J. (2018). Performance of structural concrete with recycled plastic waste as a partial replacement for sand. *Construction and Building Materials, 161*, 63–69.

Torres, A., Brandt, J., Lear, K., & Liu, J. (2017). A looming tragedy of the sand commons. *Science, 357*(6355), 970–971.

UNSCEAR (United Nations Scientific Committee on the Effects of Atomic Radiation), Sources and Effects of Ionizing Radiation. (2000). ANNEX B, exposures from natural radiation sources. *UNSCEAR 2000 REPORT, 1*, 97–99. New York.

Zhang, L., Shen, H., Xu, K., Huang, W., Wang, Y., Chen, M., & Han, B. (2023). Effect of ceramic waste tile as a fine aggregate on the mechanical properties of low-carbon ultrahigh performance concrete. *Construction and Building Materials, 370*, Article 130595.

Zhang, P., Sun, X., Wang, F., & Wang, J. (2023). Mechanical properties and durability of geopolymer recycled aggregate concrete: A review. *Polymers, 15*(3), 615.